

# Practical volume estimation by a new annealing schedule for cooling convex bodies

**Apostolos Chalkis**

Department of Informatics & Telecommunications  
National & Kapodistrian University of Athens, Greece  
achalkis@di.uoa.gr

**Ioannis Z. Emiris**

Department of Informatics & Telecommunications  
National & Kapodistrian University of Athens, Greece  
emiris@di.uoa.gr

**Vissarion Fisikopoulos**

Department of Informatics & Telecommunications  
National & Kapodistrian University of Athens, Greece  
vfisikop@di.uoa.gr

---

## Abstract

We study the problem of estimating the volume of convex polytopes, focusing on H- and V-polytopes, as well as zonotopes. Although a lot of effort is devoted to practical algorithms for H-polytopes there is no such method for the latter two representations. We propose a new, practical algorithm for all representations, which is faster than existing methods. It relies on Hit-and-Run sampling, and combines a new simulated annealing method with the Multiphase Monte Carlo (MMC) approach.

Our method introduces the following key features to make it adaptive: (a) It defines a sequence of convex bodies in MMC by introducing a new annealing schedule, whose length is shorter than in previous methods with high probability, and the need of computing an enclosing and an inscribed ball is removed; (b) It exploits statistical properties in rejection-sampling and proposes a better empirical convergence criterion for specifying each step; (c) For zonotopes, it may use a sequence of convex bodies for MMC different than balls, where the chosen body adapts to the input. We offer an open-source, optimized C++ implementation, and analyze its performance to show that it outperforms state-of-the-art software for H-polytopes by Cousins-Vempala (2016) and Emiris-Fisikopoulos (2018), while it undertakes volume computations that were intractable until now, as it is the first polynomial-time, practical method for V-polytopes and zonotopes that scales to high dimensions (currently 100).

We further focus on zonotopes, and characterize them by their order (number of generators over dimension), because this largely determines sampling complexity. The number of phases in MMC tends to constant as order increases, while the bodies in (c) are balls. For low orders, the generators' matrix is used to define a centrally symmetric convex polytope in (c). We analyze a related application, where we evaluate methods of zonotope approximation in engineering.

**2012 ACM Subject Classification** Design and analysis of algorithms:  
Computational geometry, Random walks and Markov chains

**Keywords and phrases** Polytope volume, zonotope, sampling, simulated annealing, V-polytopes

## 1 Introduction

As a special case of integration, volume computation is a fundamental problem with many applications in science and engineering. From a computational complexity point of view it is hard even if we restrict to convex sets. In particular, it is #P-hard for H- and V-polytopes, including zonotopes [13]. It is even hard to approximate, namely, APX-hard [10]. Therefore, a great effort has been devoted to randomized approximation algorithms, starting with the celebrated result in [9] with complexity  $O^*(d^{23})$ , where  $O^*(\cdot)$  indicates a soft-big-Oh hiding polylog factors. It introduced the

## 2 Practical volume estimation

Multiphase Monte Carlo (MMC) technique, which reduced volume approximation to computing a telescoping product of volumes, estimated by uniformly sampling a sequence of convex bodies (by means of random walks). The following years, improved algorithms reduced the exponent of dimension  $d$  down to 5 [17]. The latter led to the first practical implementation [11] for high dimensions, which highlighted the importance of Coordinate Direction Hit-and-Run (HnR). Further results in [6, 18] reduced the exponent to 3, followed by another practical method [7].

This paper proposes a new practical volume estimation for convex polytopes, improving upon state-of-the-art methods for H-polytopes, while yielding the first method capable to scale in the case of V-polytopes and zonotopes. We use an adaptive sequence of convex bodies, simulated annealing, and the statistical properties of the telescoping ratios in order to drastically reduce the number of phases in MMC as well as the sample size required to estimate these ratios. Our aim is to fully exploit probabilistic methods within the current paradigm of the MMC approach, and optimize the resulting software by careful algorithmic engineering.

**Notation.**  $P$  is a full-dimensional convex polytope lying in  $d$ -dimensional space. An H-polytope (in H-representation) is  $P = \{x \mid Ax \leq b, A \in \mathbb{R}^{q \times d}, b \in \mathbb{R}^q\}$ . A V-polytope is the convex hull of a pointset in  $\mathbb{R}^d$ . A zonotope (Z-polytope) is the Minkowski sum of  $k$   $d$ -dimensional segments or equivalently given by matrix  $G \in \mathbb{R}^{d \times k}$  and seen as a linear map of hypercube  $[-1, 1]^k$  to  $\mathbb{R}^d$ : we call it a Z-representation. The *order* of a zonotope is the ratio  $k/d$ . We study sequences of bodies  $C_i$  intersecting  $P$  where the corresponding convex bodies  $P_i = C_i \cap P$  define the telescoping product.

**Membership oracles.** A point  $x_0 \in P$  if and only if  $Ax_0 \leq b$  when  $P$  is a H-polytope. If  $P$  is a V-polytope we follow [12] and solve the linear program (LP) below,

$$\begin{aligned} \max f &= z^T x_0 - z_0 \\ \text{subject to } z^T v_i - z_0 &\leq 0, \text{ for all } i = 1, \dots, v \\ z^T x_0 - z_0 &\leq 1 \end{aligned}$$

The  $x_0 \in P$  holds if and only if the optimal value  $f$  of the LP is strictly positive and the LP computes a separating hyperplane. If  $P$  is a zonotope we solve the following linear feasibility problem,

$$\begin{aligned} \text{find } \lambda \\ \text{satisfying } G\lambda &= x_0 \\ -1 \leq \lambda_i &\leq 1, \text{ for all } i = 1, \dots, k \end{aligned}$$

The  $x_0 \in P$  holds if and only if the answer is positive.

**Paper structure.** The rest of the section presents previous work as well as our contributions. Section 2 discusses our method, while Section 3 presents our implementation, evaluates its practical complexity, compares to existing software and offers a concrete application.

### 1.1 Previous work

The prevalent paradigm in volume approximation relies on MMC and sampling with random walks. We build on the approach which defines a sequence of convex bodies  $P_0 \subseteq \dots \subseteq P_m = P$  such that rejection sampling would efficiently estimate  $\text{vol}(P_{i+1})/\text{vol}(P_i)$ . Assuming  $P$  is well-rounded, i.e.  $B_d \subseteq P \subseteq C\sqrt{d}B_d$ , one defines a sequence of scaled copies of the unit ball  $B_d$ , and  $P_i = (2^{i/d}B_d) \cap P$ ,  $i = 0, \dots, m$ . Then, it suffices to compute  $\text{vol}(P_0)$  and apply the following telescoping product from [17]:

$$\text{vol}(P) = \text{vol}(P_0) \frac{\text{vol}(P_1)}{\text{vol}(P_0)} \dots \frac{\text{vol}(P_m)}{\text{vol}(P_{m-1})}, \quad m = O(d \lg d)$$

In practical implementations [11], assuming  $rB_d \subseteq P \subseteq RB_d$ , the construction gives  $m = \lceil d \lg(R/r) \rceil$ , see Figure 1 (left). The critical complexity issue is to define a sequence that minimizes  $m$  while each ratio remains bounded by a constant. This would permit a larger approximation error per ratio without compromising overall error, while it would require a smaller sample.

Each ratio is estimated by sampling uniform points from  $P_i$ , obtained by random walks. The main approach today being HnR while, more recently, a convergence rate is given for Hamiltonian walk [16] applicable to H-polytopes only. The Vaidya walk is even faster [?] when the number of facets  $\gg d$ . A recent Hamiltonian walk with reflections [5] reduces mixing time: It can enhance our method for H-polytopes and may offer better stability than Coordinate Directions HnR; it can also be integrated to the two existing implementations discussed below. But its application to V- and Z-polytopes is unclear.

In [18] they construct and estimate the volume of a  $d + 1$  dimensional convex body, called the "pencil", and then they use rejection sampling to estimate the volume of the input convex body. Moreover, they generalize the telescopic product to a sequence of functions by fixing a sequence of exponential distributions approximating the uniform; the total complexity is  $O^*(d^4)$ . In [6], which holds the current record in asymptotic analysis for volume approximation of general convex bodies, they consider a sequence of spherical Gaussian distributions on  $P$ ; the total complexity is  $O^*(d^3)$ . The sequence of spherical Gaussians is not deterministic, but approaches the uniform distribution fast. In [16] they improve the asymptotic complexity to  $O^*(qd^{\frac{2}{3}})$  for H-polytopes as they combine Hamiltonian Monte Carlo with a sequence of Gibbs distributions instead of Gaussians.

Current state-of-the-art software handles H-polytopes based on the above paradigms and, typically, HnR. The software of [11] scales up to hundreds of dimensions and uses Coordinate-Direction HnR. We also juxtapose the software of [7] (for H-polytopes), implementing [6] with an annealing schedule [18] of a sequence of Gaussians. For the ratio, they use a sliding window and stop sampling when the maximum and minimum values meet a convergence criterion.

The main reason that these implementations cannot handle efficiently Z- nor V-polytopes (cannot scale beyond, say,  $d \geq 15$ ) is that the boundary and membership oracles require to solve linear programs (LPs). Moreover both of them require inscribed balls. If  $P$  is a zonotope, checking whether a ball  $B \subseteq P$  is in co-NP, but it is not known whether it is co-NP-complete. When  $P$  is a V-polytope, given  $p \in P$  the computation of the largest inscribed ball centered at  $p$  is NP-hard [19]. Additionally, the software of [7] requires the number of facets which is typically exponential in the dimension for both Z- and V-polytopes (Section 3 and Figure 6).

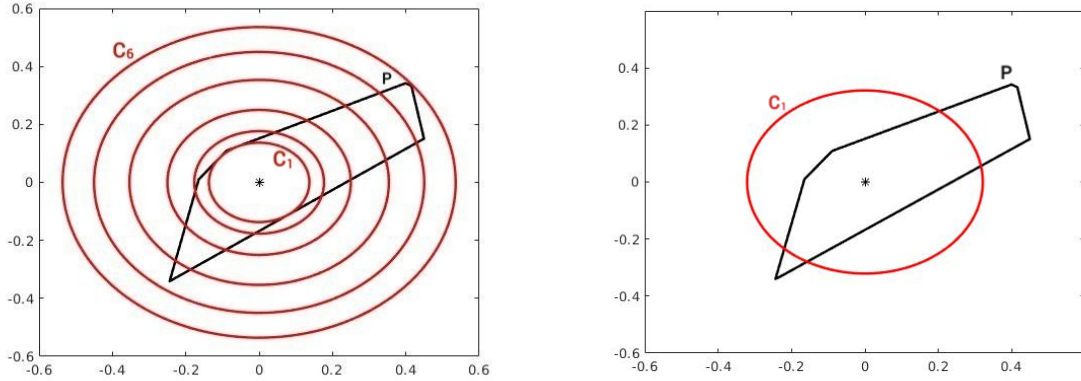
To sum up the discussion on previous work we should mention the rich area of implementations of deterministic algorithms; notable examples are VINCI and qHull but the list is quite long. As expected, those implementations do not scale beyond, say,  $d \geq 15$  dimensions for general polytopes.

For zonotopes and V-polytopes, computing the largest inscribed ball is a key issue for both methods. If  $P$  is a zonotope, checking whether a ball  $B \subseteq P$  is in co-NP, but it is not known whether it is co-NP-complete. When  $P$  is a V-polytope given  $p \in P$  the computation of the largest inscribed ball centered at  $p$  is NP-hard [19].

## 1.2 Our contribution

Our contribution is a new volume approximation method for H-, V-, and Z-polytopes, also applicable to general convex bodies, though in this paper we focus on convex polytopes. For V- and Z-polytopes, our algorithm requires solving two (related) LPs per step of the random walk (Section 2.3). However, we drastically reduce the number of such steps, hence offering the first practical algorithm for such bodies in high dimensions. Regarding LPs, each step solves two LPs with a common basic feasible solution. In Section 3 we experimentally analyze our method to show it scales up to 100 dimensions for V-polytopes and low order zonotopes. Hence, it outperforms both implementations in [11, 7] on V- and Z-polytopes (Figure 6). In fact, it performs volume computations which were

## 4 Practical volume estimation



■ **Figure 1** Balls computed by MMC in [17] (left) and by the annealing schedule of Algorithm 2 with  $r=0.25$  and  $\delta=0.05$  (right).

intractable until now (Table 2). On H-polytopes our method is faster than [11] for every  $d$  and faster for  $d \leq 100$  than [7] (Table 3 and Figure 6). The main algorithmic features follow:

- We design a new simulated annealing method for cooling convex bodies in MMC (Section 2.1). We exploit the fact that rejection sampling works efficiently for bounded ratios, which are actually smaller than those in [17] (see Figure 1). To reduce the number of phases, we employ statistical tests to bound each  $r_i = \text{vol}(P_{i+1})/\text{vol}(P_i)$  with high probability. Our annealing schedule does not need an enclosing body of  $P$  as they do in [17, 11]: it suffices to set  $P_0 = P$ . In addition, our method does not require computing an inscribed ball, as older methods did: the ball (or any body we use in MMC) with minimum volume is computed by the annealing schedule, thus further reducing the number of phases in practice. Finally, we prove that the annealing schedule terminates successfully with constant probability (Section 2.1). This adaptive MMC sequence reduces significantly the number of phases: we prove that this number in [17, 11] upper bounds the number of phases in our method with high probability (Section 2.4).
- When we sample  $N$  uniform points from  $P_i$ , the number of points in  $P_{i+1}$  follows the binomial distribution. The main task here is to estimate the ratio  $\text{vol}(P_{i+1})/\text{vol}(P_i)$  with minimum  $N$ . We exploit the binomial proportion confidence interval and modify it by using the standard deviation of a sliding window, in order to specify a new empirical convergence criterion for the ratio, as  $N$  increases (Section 2.2); this drastically reduces sample size (Figure 6). An analogous technique was used in [7], but the window here is of half the length.
- We allow other convex bodies besides balls in MMC, the choice being a function of the input, aiming at reducing the number of phases. For H- and V-polytopes we actually use balls as in classical MMC. We leave it as an open question whether there are more suitable bodies such as those defined in [2]. For zonotopes we show that, as order grows, most suitable is the ball: our method requires only a small constant number of them (Figure 3 and Table 2). However, for low order, e.g.  $\leq 4$ , we use the matrix of generators to define a centrally-symmetric H-polytope that accelerates the algorithm so as to scale to, say,  $d = 100$ , which used to be intractable (Section 2.5). For instance, for a random zonotope with  $k = 2d$  generators,  $d = 100$ , our software takes  $< 10$  hr (Table 2).

We prove that, in our method, the number of phases is  $m = O(\lg(\text{vol}(P)/\text{vol}(B_d)))$  with high probability (Section 2.4), when we use balls in MMC. This yields  $m = O(d)$  for some well-rounded polytopes such as the cross polytopes, a clear improvement over the general bound of  $O(d \lg d)$  [17]. Specifically, for a cross V-polytope in  $d = 100$  our method requires just two balls and takes 406 sec (Figure 5 and Table 1), while the problem is intractable under the H-representation. Moreover,

when applying a rounding step to random V-polytopes our method requires very small  $m$ , in practice  $\leq 4$ , even for  $d = 100$  (Section 3, and Table 1). If  $P$  is a zonotope, we experimentally show that, for constant  $d$ , and  $k$  (number of generators) increasing, the number of phases  $m$  decreases to 1 (Table 2 and Figure 3). An intuitive property of zonotopes is that, while order increases for constant  $d$ , a random zonotope approximates the hypersphere. In [3] they prove that for  $d \geq 2$  the unit ball  $B_d$  can be approximated up to  $\epsilon$  in the Hausdorff distance by a zonotope defined by  $k$  segments of equal length,  $k \leq c(d)(\epsilon^2 |\lg \epsilon|)^{(d-1)/(d+2)}$ , where  $c(d)$  is a constant. This result cannot be used straightforwardly to prove our claim but strengthens it intuitively. For some instances, when order is large, our method creates just one ball and the method reduces to just one or two rejection-sampling steps (Table 2).

Last but not least, we offer an open source efficient implementation of the new method in C++<sup>1</sup>.

## 2 Volume algorithm

Our volume algorithm relies on Multiphase Monte Carlo (MMC) method and samples from uniform target distribution with Hit-and-Run (HnR) random walk. Hence, the first part of the algorithm (Algorithm 1) is to construct a sequence of convex bodies  $C_1 \supseteq \dots \supseteq C_m$  intersecting the given polytope  $P$  using simulated annealing (Algorithm 2). Then it estimates each ratio in the telescopic product of Equation (1) using HnR and a new empirical criterion convergence (Algorithm 3). A typical choice for the  $C_i$ 's is a sequence of co-centric balls but other convex bodies may be used (see, e.g., Section 2.5). Then,

$$\text{vol}(P) = \frac{\frac{\text{vol}(P_m)}{\text{vol}(C_m)}}{\frac{\text{vol}(P_1)}{\text{vol}(P_0)} \frac{\text{vol}(P_2)}{\text{vol}(P_1)} \dots \frac{\text{vol}(P_m)}{\text{vol}(P_{m-1})}} \text{vol}(C_m), \quad \text{where } P_0 = P, P_i = C_i \cap P. \quad (1)$$

In the sequel, we write  $r_i = \text{vol}(P_{i+1})/\text{vol}(P_i)$ ,  $i = 0, \dots, m-1$  and  $r_m = \text{vol}(P_m)/\text{vol}(C_m)$ .

---

### Algorithm 1 VolumeAlgorithm ( $P, \epsilon, r, \delta, \alpha, \nu, N, k$ )

---

```

Construct convex body  $C \subseteq \mathbb{R}^d$  s.t.  $C \cap P \neq \emptyset$  and set interval  $[q_{\min}, q_{\max}]$ 
 $\{P_0, \dots, P_m, C_m\} = \text{AnnealingSchedule}(P, C, r, \delta, \alpha, \nu, N, q_{\min}, q_{\max})$ 
Set  $\epsilon_i$ ,  $i = 0, \dots, m$  s.t.  $\sum_{i=0}^m \epsilon_i^2 = \epsilon^2$ 
for  $i = 0, \dots, m$  do
  if  $i < m$  then
     $r_i = \text{EstimateRatio}(P_i, P_{i+1}, \epsilon_i, m, k)$ 
  else
     $r_m = \text{EstimateRatio}(C_m, P_m, \epsilon_m, m, k)$ 
  end if
end for
return  $\text{vol}(C_m)/r_0/\dots/r_{m-1} \cdot r_m$ 

```

---

The behavior of Algorithm 1 is parameterized by: the error of approximation  $\epsilon$ , cooling parameters  $0 < r + \delta < 1$ ,  $r, \delta > 0$ , which are used in the schedule, significance level (s.l.)  $\alpha > 0$  of the statistical tests,  $\nu$  the degrees of freedom for the t-student used in t-tests (all in Section 2.1), and parameter  $N$  that controls the number of points  $\nu N$  generated in  $P_i$ . We generate uniform samples in  $P_i$  using HnR (Section 2.3).

Following the telescopic product of Equation (1), it is clear that in practical estimations  $C_m$  has to be a convex body whose volume is obtained much faster than  $\text{vol}(P)$  (ideally by a closed formula)

<sup>1</sup> [https://github.com/GeomScale/volume\\_approximation/tree/CoolingBodies](https://github.com/GeomScale/volume_approximation/tree/CoolingBodies)

## 6 Practical volume estimation

and easy to sample. The maximum number of constructed convex bodies by Algorithm 1 can be bounded by upper and lower probabilistic bounds (Section 2.4). When the input is a zonotope we study other choices for the sequence of bodies, i.e. sequences of balls and H-polytopes (Section 2.5).

### 2.1 Annealing schedule for convex bodies

Given a convex polytope  $P$ , an error parameter  $\epsilon$  and  $r, \delta, \alpha$  s.t.  $0 < r + \delta < 1$ , the annealing schedule (Algorithm 2) generates the sequence of convex bodies  $C_1 \supseteq \dots \supseteq C_m$  defining  $P_i = C_i \cap P$ ,  $i = 1, \dots, m$  and  $P_0 = P$ . The main goal is to restrict each ratio  $r_i$  in the interval  $[r, r + \delta]$  with high probability. We call  $r, \delta$  cooling parameters and  $\alpha$  the significance level (s.l.) of the schedule.

We introduce some notions from statistics needed to define two tests and refer to [8] for details. Given  $\nu$  observations from a r.v.  $X \sim \mathcal{N}(\mu, \sigma^2)$  with unknown variance  $\sigma^2$ , the (one tailed) t-test checks the null hypothesis that the population mean exceeds a specified value  $\mu_0$  using the statistic  $t = \frac{\bar{x} - \mu_0}{s/\sqrt{\nu}} \sim t_{\nu-1}$ , where  $\bar{x}$  is the sample mean,  $s$  the sample standard deviation and  $t_{\nu-1}$  is the t-student distribution with  $\nu - 1$  degrees of freedom. Given a s.l.  $\alpha > 0$  we test the null hypothesis for the mean value of the population,  $H_0 : \mu \leq \mu_0$  against  $H_1 : \mu > \mu_0$ . We reject  $H_0$  if,

$$t \geq t_{\nu-1, \alpha} \Rightarrow \bar{x} \geq \mu_0 + t_{\nu-1, \alpha} s / \sqrt{\nu},$$

which implies  $\Pr(\text{reject } H_0 \mid H_0 \text{ true}) = \alpha$ . Otherwise we fail to reject  $H_0$ . The schedule algorithm uses the following two statistical tests:

<p><b>testL</b>(<math>P_1, P_2, r, \delta, \alpha, \nu, N</math>):  <math>H_0 : \text{vol}(P_2)/\text{vol}(P_1) \geq r + \delta</math>  <math>H_1 : \text{vol}(P_2)/\text{vol}(P_1) \leq r + \delta</math>  <b>Successful if <math>H_0</math> is rejected</b></p>	<p><b>testR</b>(<math>P_1, P_2, r, \alpha, \nu, N</math>):  <math>H_0 : \text{vol}(P_2)/\text{vol}(P_1) \leq r</math>  <math>H_1 : \text{vol}(P_2)/\text{vol}(P_1) \geq r</math>  <b>Successful if <math>H_0</math> is rejected</b></p>
---	---

They are used to restrict each  $r_i$  to  $[r, r + \delta]$ . In the sequel we write **testL**( $P_1, P_2$ ) and **testR**( $P_1, P_2$ ).

If we sample  $N$  uniform points from a body  $P_i$  then r.v.  $X$  that counts points in  $P_{i+1}$ , follows  $X \sim b(N, r_i)$ , the binomial distribution and  $Y = X/N \sim \mathcal{N}(r_i, r_i(1 - r_i)/N)$  is Gaussian.

► **Remark.** This normal approximation suffices when  $N$  is large enough and we adopt the well known rule of thumb to use it only if  $Nr_i(1 - r_i) > 10$ .

Then each sample proportion that counts successes in  $P_{i+1}$  over  $N$  is an unbiased estimator for the mean of  $Y$ , which is  $r_i$ . So if we sample  $\nu N$  points from  $P_i$  and split the sample into  $\nu$  sublists of length  $N$ , the corresponding  $\nu$  ratios are experimental values that follow  $\mathcal{N}(r_i, r_i(1 - r_i)/N)$  and can be used to check both null hypotheses in **testL** and **testR**. So, using the mean  $\hat{\mu}$  of the ratios, assuming

$$r + \delta - t_{\nu-1, \alpha} \frac{s}{\sqrt{\nu}} \geq \hat{\mu} \geq r + t_{\nu-1, \alpha} \frac{s}{\sqrt{\nu}},$$

then  $r_i$  is restricted to  $[r, r + \delta]$  with high probability. Details and bounds on the number of phases are given in Section 2.4.

<p><b>Perform testR and testL</b>  <b>Input:</b> convex bodies <math>P_1, P_2</math>, cooling parameters <math>r, \delta</math>, significance level <math>\alpha</math> and <math>\nu, N \in \mathbb{N}</math></p> <hr style="width: 25%; margin-left: 0;"/> <p>Sample <math>\nu N</math> uniform points from <math>P_1</math>            Partition <math>\nu N</math> points to lists <math>S_1, \dots, S_\nu</math>, each of length <math>N</math>            Compute ratios <math>\hat{r}_i =  \{q \in P_2 : q \in S_i\}  / N</math>, <math>i = 1, \dots, \nu</math>            Compute the mean, <math>\hat{\mu}</math>, and standard deviation, <math>s</math>, of the <math>\nu</math> ratios</p>
---

**if**  $\hat{\mu} \geq r + t_{\nu-1, \alpha} \frac{s}{\sqrt{\nu}}$  **then** **testR** holds, **otherwise** **testR** fails  
**if**  $\hat{\mu} \leq r + \delta - t_{\nu-1, \alpha} \frac{s}{\sqrt{\nu}}$  **then** **testL** holds, **otherwise** **testL** fails

Let us now describe the annealing schedule: Each body  $C_i$  in  $C_1 \supseteq \dots \supseteq C_m$  is a scalar multiple of a given body  $C$ . When  $C$  is the unit ball, the body used in each step is determined by a radius. Since our algorithm does not use an inscribed ball, the initialization step computes the body with minimum volume, denoted by  $C'$  or  $C_m$ , s.t.  $r_m \in [r, r + \delta]$  with high probability. The algorithm employs  $C'$  to decide stopping at the  $i$ -th step; if the criterion fails, the algorithm computes  $P_{i+1}$  by a regular step.

**Initialization step.** The schedule is given convex body  $C$ , and an interval  $[q_{\min}, q_{\max}]$ . At initialization, one computes  $q \in [q_{\min}, q_{\max}]$  s.t. both **testL**( $qC, qC \cap P$ ) and **testR**( $qC, qC \cap P$ ) are successful. Now  $q_{\min}C$  corresponds to a body that fails in **testR** with unit probability, e.g. when  $q_{\min}C \subseteq P$ , while  $q_{\max}C$  to one for which **testL** fails with probability arbitrarily close to 1. The computation of  $q_{\min}, q_{\max}$  is not trivial but in Section 3 we give practical selections depending on body  $C$  which are very efficient in practice.

The algorithm performs binary search in  $[q_{\min}, q_{\max}]$ . Let  $q = (q_{\min} + q_{\max})/2$  then:

1. If **testL**( $qC, qC \cap P$ ) succeeds and **testR**( $qC, qC \cap P$ ) fails, continue to the left-half of the interval.
2. If **testL**( $qC, qC \cap P$ ) fails and **testR**( $qC, qC \cap P$ ) succeeds, continue to the right-half of the interval.
3. If both **testL**( $qC, qC \cap P$ ) and **testR**( $qC, qC \cap P$ ) succeed, stop and set  $C' = qC$ .
4. If both **testL**( $qC, qC \cap P$ ) and **testR**( $qC, qC \cap P$ ) fail (contradiction) then sample a new set of  $\nu N$  uniform points from  $qC$  and repeat both tests.

Note that in each step of binary search, the schedule samples  $\nu N$  points from  $qC$  to check both **testL** and **testR**. The output is  $C'$  which shall be denoted by  $C_m$  at termination.

---

**Algorithm 2** AnnealingSchedule ( $P$ , body  $C$ ,  $r$ ,  $\delta$ ,  $\alpha$ ,  $\nu$ ,  $N$ ,  $q_{\min}$ ,  $q_{\max}$ )

---

```

 $q_1 = q_{\min}, q_2 = q_{\max}, q = (q_1 + q_2)/2$ 
loop of the binary search for the initialization:
   $C' = qC$ 
  if testR( $C', C' \cap P$ ) and testL( $C', C' \cap P$ ) succeed stop loop
  if testR( $C', C' \cap P$ ) succeeds and testL( $C', C' \cap P$ ) fails set  $q_1 = q, q = (q_1 + q_2)/2$ 
  if testR( $C', C' \cap P$ ) fails and testL( $C', C' \cap P$ ) succeeds set  $q_2 = q, q = (q_1 + q_2)/2$ 
  if testR( $C', C' \cap P$ ) and testL( $C', C' \cap P$ ) fail sample  $\nu N$  new uniform points from  $C'$ 
end loop
set  $P_0 = P, i = 0, q_{\min} = q$ 
loop for the definition of the sequence
   $q_1 = q_{\min}, q_2 = q_{\max}, q = (q_1 + q_2)/2$ 
  if testR( $P_i, C' \cap P$ ) succeeds set  $m = i + 1, P_m = C' \cap P$  and stop loop
  loop of the binary search to define  $P_{i+1}$ 
     $P' = qC \cap P$ 
    if both testR( $P_i, P'$ ) and testL( $P_i, P'$ ) succeed set  $P_{i+1} = P', i = i + 1$  stop loop
    if testR( $P_i, P'$ ) succeeds and testL( $P_i, P'$ ) fails set  $q_2 = q, q = (q_1 + q_2)/2$ 
    if testR( $P_i, P'$ ) fails and testL( $P_i, P'$ ) succeeds set  $q_1 = q, q = (q_1 + q_2)/2$ 
    if testR( $C', C' \cap P$ ) and testL( $C', C' \cap P$ ) fail sample  $\nu N$  new uniform points from  $P_i$ 
  end loop
   $q_{\max} = q$ 
end loop
return  $\{P_0, \dots, P_m, C'\}$ 

```

---



## 8 Practical volume estimation

**Regular step.** At step  $i$ , the algorithm determines  $P_{i+1}$  by computing a scaling factor of  $C$  s.t. volume ratio  $r_i \in [r, r + \delta]$  with high probability. The schedule samples  $\nu N$  points from  $P_i$  and binary searches for a  $q_{i+1}$  in an updated interval  $[q_{\min}, q_{\max}]$  s.t. both  $\text{testL}(P_i, q_{i+1}C \cap P)$  and  $\text{testR}(P_i, q_{i+1}C \cap P)$  are successful. Then set  $P_{i+1} = q_{i+1}C \cap P$ . To update the interval, Algorithm 2 uses the  $q$  value of  $C'$  computed in the initialization step as  $q_{\min}$  and the  $q$  value of  $P_i$  computed in the previous step as  $q_{\max}$ . The updated interval implies that  $\text{vol}(P_{i+1})$  has to lie between  $\text{vol}(P_i)$  and  $\text{vol}(C' \cap P)$ .

**Stopping criterion.** The algorithm uses  $C' \cap P$  in the  $i$ -th step for checking whether  $\text{vol}(P_i)/\text{vol}(C' \cap P) \geq r$  with high probability, using only  $\text{testR}$ . Formally,  $C' \cap P$  is the body with minimum volume in the sequence:

*Stop in step  $i$  if  $\text{testR}(P_i, C' \cap P)$  holds. Then, set  $m = i + 1$ , and  $P_m = C' \cap P$ .*

To perform  $\text{testR}$ ,  $\nu N$  points are sampled from  $P_i$ . The schedule stops when  $\text{vol}(C' \cap P)/\text{vol}(P_i)$  is large enough according to  $\text{testR}$ . It is clear that, at termination,  $C_m = C'$ . Otherwise, the algorithm determines the next convex body  $P_{i+1}$  in a regular step.

**Termination.** We demonstrate halting of Algorithm 2 for a given input polytope  $P$  and a set of parameters. Before stating the theorem, let us introduce the notion of the power of a t-test:  $\text{pow} = \Pr[\text{reject } H_0 \mid H_0 \text{ false}] = 1 - \beta$ . The power of a t-test cannot be usually calculated in practice. It is well known that it depends on s.l.  $\alpha$ , sample size  $\nu$ , and the magnitude of the effect on the mean value of the population. For example, for  $\text{testR}$ , assuming  $r_i = \theta > r$ , we have

$$\text{pow}(\theta) = \Pr \left[ \frac{\hat{\mu} - r}{s/\sqrt{\nu}} > t_{\nu-1, \alpha} \mid r_i = \theta \right] = 1 - F_{t_{\nu-1}}^{-1} \left( t_{\nu-1, \alpha} - \frac{\theta - r}{s/\sqrt{\nu}} \right) = 1 - \beta,$$

where  $F_{t_{\nu-1}}^{-1}$  is the quantile function of t-student with  $\nu - 1$  degrees of freedom. A similar analysis for the power of  $\text{testL}$  is straightforward.

In the t-tests of Algorithm 2 we might have some errors of type I or II and, thus, binary search in intervals that do not contain values corresponding to ratios in  $[r, r + \delta]$ . Therefore, there is a probability that Algorithm 2 fails to terminate. The following theorem states that this probability is bounded by a constant when Algorithm 2 performs at least as many steps as the minimum number required for it to terminate: this number is denoted by  $Q$ , depends on the inputs, and occurs when there are no errors in the performed t-tests.

► **Theorem 1.** Let Algorithm 2 perform some number  $M \geq Q$  of steps. Let  $\beta_{\max}, \beta_{\min}$  be the maximum and the minimum among all the values of the quantile function in the  $M$  pairs of t-tests of  $\text{testL}$  and  $\text{testR}$  respectively. Then Algorithm 2 terminates with constant probability, namely:

$$\Pr[\text{Algorithm 2 terminates}] \geq 1 - 2 \frac{\alpha(1 - \beta_{\min}) + \beta_{\max}}{1 - \alpha(1 - \beta_{\min}) + \beta_{\max}} - \frac{2\beta_{\max} - \beta_{\min}^2}{1 - 2\beta_{\max} - \beta_{\min}^2}.$$

**Proof.** Let  $M \geq Q$ . If Algorithm 2 fails to terminate after  $M$  pairs of  $\text{testL}$  and  $\text{testR}$ , then some type I or type II error occurred in the t-tests. An error of type I occurs when the null Hypothesis is true and the test rejects it, while type II occurs when the null Hypothesis is false and the test fails to reject it. The respective probabilities are  $\Pr[\text{reject } H_0 \mid H_0 \text{ true}] = \alpha$  and  $\Pr[\text{fail to reject } H_0 \mid H_0 \text{ false}] = \beta$ , which is a value of the quantile function of t-student. For the latter probability we write  $\beta_L, \beta_R$  for  $\text{testL}$  and  $\text{testR}$  respectively. If, for a pair of tests, both null hypotheses are false then an error occurs with probability

$$\begin{aligned} p_1 &= \Pr[\text{error occurs} \mid \text{both } H_0 \text{ false}] = \beta_L(1 - \beta_R) + \beta_R(1 - \beta_L) + \beta_L\beta_R \\ &= \beta_L + \beta_R - \beta_L\beta_R \leq 2\beta_{\max} - \beta_{\min}^2 \end{aligned}$$



Similarly,

$$\begin{aligned} p_2 &= \Pr[\text{error occurs} \mid \text{testL } H_0 \text{ false and testR } H_0 \text{ true}] = \\ &= \alpha(1 - \beta_L) + \alpha\beta_L + \beta_L(1 - \alpha) \\ &= \alpha + \beta_L - \alpha\beta_L \leq \alpha + \beta_{\max} - \alpha\beta_{\min} \end{aligned}$$

$$\begin{aligned} p_3 &= \Pr[\text{error occurs} \mid \text{testR } H_0 \text{ false and testL } H_0 \text{ true}] = \\ &= \alpha(1 - \beta_R) + \alpha\beta_R + \beta_R(1 - \alpha) \\ &= \alpha + \beta_R - \alpha\beta_R \leq \alpha + \beta_{\max} - \alpha\beta_{\min} \end{aligned}$$

Then,

$$\begin{aligned} \Pr[\text{Algorithm 2 fails to terminate}] &\leq \sum_{i=1}^M p_1^i + \sum_{i=1}^M p_2^i + \sum_{i=1}^M p_3^i \leq \sum_{i=1}^{\infty} p_1^i + \sum_{i=1}^{\infty} p_2^i + \sum_{i=1}^{\infty} p_3^i \\ &= \frac{1}{1 - p_1} + \frac{1}{1 - p_2} + \frac{1}{1 - p_3} - 3 \\ &\leq 2 \frac{\alpha(1 - \beta_{\min}) + \beta_{\max}}{1 - \alpha(1 - \beta_{\min}) + \beta_{\max}} + \frac{2\beta_{\max} - \beta_{\min}^2}{1 - 2\beta_{\max} - \beta_{\min}^2}. \end{aligned}$$

◀

## 2.2 Empirical ratio estimation

As described in the previous section, annealing schedule returns  $m$  bodies intersecting  $P$  that is we estimate  $m + 1$  ratios in total. In this section we describe how this estimation is performed. First, we bound the error in the estimation of each ratio in order to use it for the definition of the stopping criterion. For each ratio  $r_i$ , we bound error by  $\epsilon_i$  s.t.

$$\sum_{i=0}^m \epsilon_i^2 = \epsilon^2 \tag{2}$$

then, from standard error propagation analysis, Equation (1) estimates  $\text{vol}(P)$  with error at most  $\epsilon$ . In section 3 we discuss efficient error splitting in practical implementations.

For fixed step  $i$  of the schedule, and for each new sample point generated in  $P_i$ , we update and keep the value of the  $i$ -th ratio. If we assume uniform sampling then the number of points in  $P_{i+1}$  follows the binomial distribution  $b(n, r_i)$ , where  $n$  is the number of points we have generated in  $P_i$ . Then a confidence interval of  $r_i$  is given by

$$\hat{r} \pm z_{\alpha/2} \sqrt{\frac{\hat{r}(1 - \hat{r})}{n}} \tag{3}$$

where  $\hat{r}$  is the proportion of the number of points in  $P_{i+1}$  over  $n$  and  $z_{\alpha/2}$  is the  $1 - \alpha/2$  quintile of the Gaussian distribution. Notice that while  $n$  increases the interval is becoming tighter around  $\hat{r}$  so that a natural choice is to stop when  $z_{\alpha/2} \sqrt{\frac{\hat{r}(1 - \hat{r})}{n}} \left/ \left( \hat{r} - z_{\alpha/2} \sqrt{\frac{\hat{r}(1 - \hat{r})}{n}} \right) \leq \epsilon_i \right.$  and to sample  $O(1/\epsilon_i^2)$  points from  $P_i$ . Then Equation (1) would estimate  $\text{vol}(P)$  up to at most  $\epsilon$  error with probability  $(1 - \alpha)^{m+1}$ . In practice we generate approximate uniform samples which makes that criterion completely useless, because for small random walk steps the number of points we obtain in  $P_{i+1}$  do not follow the binomial distribution and the criterion usually results to false positives.

Recall that the quantity  $\sqrt{\hat{r}(1 - \hat{r})/n}$  is an estimator of the standard deviation of all the sample proportions of size  $n$ . In our empirical criterion we replace that quantity with the standard deviation of a sliding window, which stores consecutive estimators of  $r_i$ . In particular, we store the last  $k$

**Algorithm 3** EstimateRatio( $P_1, P_2, e, m, k$ )

---

```

set  $p = 1 - \sqrt[m+1]{3/4}$ ,  $convergence = false$ ,  $j = 0$ ,  $count\_in = 0$ , sliding window  $W$  of length  $k$ 
while  $convergence == false$  do
   $j = j + 1$ 
  Get a uniform point  $q_j$  from  $P_1$ 
  if  $q_j \in P_2$  then
     $count\_in = count\_in + 1$ 
  end if
   $\hat{r} = \frac{count\_in}{j}$ 
  if  $W$  is full then remove  $W_1$ 
  store  $\hat{r}$  to  $W$ 
  if  $j > k$  then
    set  $s = std(W)$ ,  $a = \hat{r} - z_{p/2}s$ ,  $b = \hat{r} + z_{p/2}s$ 
    if  $(b - a)/a \leq e/2$  then
       $convergence = true$ 
    end if
  end if
end while
return  $\hat{r}$ 

```

---

ratios in a queue called sliding window denoted by  $W$  and we say that  $W$  has length  $k$ . We update  $W$  each time a new sample point is generated by inserting the new value of the  $i$ -th ratio and by popping out the oldest ratio value in  $W$ . We stop sampling when  $\hat{r}$  and the st.d. of the values in  $W$ , called  $s$ , meet the criterion of Equation (4): they we say they meet convergence. Clearly, for the first  $k$  points sampled in  $P_i$ , we do not check for convergence. Let  $p = 1 - \sqrt[m+1]{3/4}$  and the criterion is as follows:

$$\text{If } \frac{(\hat{r} + z_{p/2}s) - (\hat{r} - z_{p/2}s)}{\hat{r} - z_{p/2}s} = \frac{2z_{p/2}s}{\hat{r} - z_{p/2}s} \leq \frac{\epsilon_i}{2}, \text{ then declare convergence.} \quad (4)$$

The size  $k$  of the sliding window is determined experimentally (Section 3).

### 2.3 Sampling

We use HnR with uniform target distribution for sampling from  $P_i$  at step  $i$  of the annealing schedule or ratio estimation. With  $\ell$  directed along a random vector on the boundary of the  $d$ -dimensional unit hypersphere, we have Random Direction HnR (RDHR). If  $\ell$  is defined by a random vector parallel to one of the axes, we have Coordinate Direction HnR (CDHR). If  $P$  is given as a set of  $m$  inequalities, RDHR costs  $O(md)$  and CDHR  $O(m)$  per step. For zonotopes each step in both CDHR and RDHR solves the following LP to compute one extreme point on  $\ell \cap P$ :

$$\min \alpha, \text{ s.t. } p + \alpha v = \sum_{i=1}^k \lambda_i g_i \quad -1 \leq \lambda_i \leq 1. \quad (5)$$

For the second extreme point, keep the same constraints and minimize  $-\alpha$ . This LP uses the basic feasible solution of the first one. For V-polytopes we use the same LP with constraint  $0 \leq \lambda_i \leq 1$  and  $\sum_{i=1}^v \lambda_i = 1$  while  $g_i$  equals the  $i$ -th vertex. In Section 3 we discuss practical choices of the walk step.

## 2.4 Number of phases

In this section we give probabilistic bounds for the number of phases. To do this, we assume that i) polytope  $P$  is sandwiched,  $rB_d \subseteq P \subseteq RB_d$ , ii) we sample uniform points in each step of Algorithm 2 and iii) that Algorithm 2 terminates successfully. The construction in [17] defines a sequence of convex bodies of length  $m = \lceil \lg(\text{vol}(RB_d)/\text{vol}(rB_d)) \rceil = \lceil d \lg(R/r) \rceil$  and each ratio is restricted  $\frac{1}{2} \leq \text{vol}(K_i)/\text{vol}(K_{i+1}) \leq 1$ . If  $P$  is well-rounded then  $m = O(d \lg d)$ . In our method we can use any convex body for the sandwiching. Moreover we give a corollary which states which convex body minimizes the number of phases for a given input  $P$ .

► **Proposition 2.** Given  $P \subset \mathbb{R}^d$  and cooling parameters  $r, \delta$  s.t.  $r + \delta < 1/2$  and parameters  $\alpha, N, \nu, q_{\min}, q_{\max}$  let  $m$  be the number of convex bodies in MMC returned by Algorithm 2. Then  $\Pr[m \leq \lceil d \lg(R/r) \rceil] \geq 2 - \frac{1}{1-\gamma} = 1 - \frac{\gamma}{1-\gamma}$ , where  $\gamma = \alpha(1 - \beta_{\min})$  and  $\beta_{\min}$  is the minimum among all the values of the quantile function appearing in **testR**.

**Proof.** If  $m > \lceil d \lg(R/r) \rceil$  holds then  $k \geq 1$  type I errors of **testL** occurred in Algorithm 2, i.e.  $H_0$  holds but the test rejects it, while **testR** was successful, i.e.  $H_0$  is false and the test rejects it. Type I error occurs with probability  $\alpha$  and the probability of the success of **testR** is  $1 - \beta_R$ . Let  $\beta_{\min}$  be the minimum among the values of the quantile function appearing in all instances of **testR**. Then,

$$\Pr[m > \lceil d \lg(R/r) \rceil] \leq \sum_{i=1}^k (a(1 - \beta_i))^i \leq \sum_{i=1}^{\infty} (a(1 - \beta_{\min}))^i = \frac{1}{1 - \alpha(1 - \beta_{\min})} - 1 \Rightarrow$$

$$\Pr[m \leq \lceil d \lg(R/r) \rceil] \geq 2 - \frac{1}{1 - \alpha(1 - \beta_{\min})} = 1 - \frac{\gamma}{1 - \gamma}, \quad \text{where } \gamma = \alpha(1 - \beta_{\min}).$$

◀

Proposition 2 implies that the number of phases in [17] upper bounds the number of phases in Algorithm 1 with high probability.

► **Proposition 3.** Given  $P \subset \mathbb{R}^d$  and cooling parameters  $r, \delta$  s.t.  $r + \delta < 1/2$  and parameters  $\alpha, N, \nu, q_{\min}, q_{\max}$  let  $m$  be the number of convex bodies in MMC returned by Algorithm 2. Then  $\Pr \left[ \left[ \log_{\frac{1}{r+\delta}} \left( \frac{\text{vol}(P)}{\text{vol}(P_m)} \right) \right] \leq m \leq \left[ \log_{\frac{1}{r}} \left( \frac{\text{vol}(P)}{\text{vol}(P_m)} \right) \right] \right] \geq 1 - \frac{\gamma_L}{1-\gamma_L} - \frac{\gamma_R}{1-\gamma_R}$ , where  $\gamma_L = \alpha(1 - \beta_{\min}^L)$ ,  $\gamma_R = \alpha(1 - \beta_{\min}^R)$  and  $\beta_{\min}^R, \beta_{\min}^L$  are the minimum among all the values of quantile function appearing in **testL** and **testR** respectively.

**Proof.**

$$\Pr \left[ \left[ \log_{\frac{1}{r+\delta}} \left( \frac{\text{vol}(P)}{\text{vol}(P_m)} \right) \right] \leq m \leq \left[ \log_{\frac{1}{r}} \left( \frac{\text{vol}(P)}{\text{vol}(P_m)} \right) \right] \right]$$

$$= 1 - \Pr \left[ m > \left[ \log_{\frac{1}{r}} \left( \frac{\text{vol}(P)}{\text{vol}(P_m)} \right) \right] \text{ or } m < \left[ \log_{\frac{1}{r+\delta}} \left( \frac{\text{vol}(P)}{\text{vol}(P_m)} \right) \right] \right]$$

$$= 1 - \Pr \left[ m > \left[ \log_{\frac{1}{r}} \left( \frac{\text{vol}(P)}{\text{vol}(P_m)} \right) \right] \right] - \Pr \left[ m < \left[ \log_{\frac{1}{r+\delta}} \left( \frac{\text{vol}(P)}{\text{vol}(P_m)} \right) \right] \right]$$

Similar to the proof of Proposition 2,  $\Pr \left[ m > \left[ \log_{\frac{1}{r}} \left( \frac{\text{vol}(P)}{\text{vol}(P_m)} \right) \right] \right] \leq \frac{\gamma_R}{1-\gamma_R}$ , where  $\gamma_R = \alpha(1 - \beta_{\min}^R)$  and  $\beta_{\min}^R$  is the minimum among all the values of quantile function appearing in **testR**. If  $m < \left[ \log_{\frac{1}{r+\delta}} \left( \frac{\text{vol}(P)}{\text{vol}(P_m)} \right) \right]$  holds then  $k \geq 1$  type I errors of **testR** occurred, while **testL** was successful with probability  $1 - \beta$ . Then,  $\Pr \left[ m < \left[ \log_{\frac{1}{r+\delta}} \left( \frac{\text{vol}(P)}{\text{vol}(P_m)} \right) \right] \right] \leq \frac{\gamma_L}{1-\gamma_L}$ , where  $\gamma_L = \alpha(1 - \beta_{\min}^L)$  and  $\beta_{\min}^L$  is the minimum among all the values of quantile function appearing in **testL**. Then

$$\Pr \left[ \left[ \log_{\frac{1}{r+\delta}} \left( \frac{\text{vol}(P)}{\text{vol}(P_m)} \right) \right] \leq m \leq \left[ \log_{\frac{1}{r}} \left( \frac{\text{vol}(P)}{\text{vol}(P_m)} \right) \right] \right] \geq 1 - \frac{\gamma_L}{1 - \gamma_L} - \frac{\gamma_R}{1 - \gamma_R}$$



From Proposition 3 it is easily derived that the number of phases in Algorithm 1 is  $m = O(\lg(\text{vol}(P)/\text{vol}(P_m)))$  with high probability. If we use balls in MMC and assume that  $rB_d \subseteq P$  then  $m = O(\lg(\text{vol}(P)/\text{vol}(rB_d)))$  which is always smaller, due to a constant, than the number of phases in [17]. As we mentioned, there are well-rounded convex bodies that our method improves this bound by  $\lg d$ , e.g. for the cross polytope  $m = O(d)$ , as  $\text{vol}(P) = 2^d/d!$ . We leave it as an open question if this result can be extended to other convex bodies. Proposition 3 also shows the importance of the type of body  $C$ .

► **Corollary 4.** Given  $P$ , the body  $C$  that minimizes the number of phases of Algorithm 1, with probability  $p \geq 1 - \frac{\gamma_L}{1-\gamma_L} - \frac{\gamma_R}{1-\gamma_R}$  for given cooling parameters  $r, \delta$  and s.l.  $\alpha$ , is the one that maximizes  $\text{vol}(C_m \cap P)$  in the annealing schedule of Algorithm 2.

## 2.5 Multiphase Monte Carlo for zonotopes

In this section we study different types of convex bodies used in the MMC sequence to approximate the volume of a zonotope, i.e. the Minkowski sum of segments. Let  $k > d$  be the number of generators of zonotope  $P \subset \mathbb{R}^d$ , and  $G$  the  $d \times k$  matrix they define. Note  $G^T G$  has  $k - d$  zero eigenvalues; the corresponding eigenvectors form  $Q \in \mathbb{R}^{k \times (k-d)}$ . The intersection of the hypercube  $[-1, 1]^k$  with the  $d$ -dimensional affine subspace defined by  $Q^T = 0$  equals a  $d$ -dimensional polytope  $C'$  in  $\mathbb{R}^k$ . SVD yields an orthonormal basis for the linear constraints, and its orthogonal complement  $W_\perp$ :

$$Q = USV^T = \begin{bmatrix} W \\ W_\perp \end{bmatrix}^T \begin{bmatrix} S_1 & 0 \\ 0 & 0 \end{bmatrix} V^T$$

Let  $Ay \leq b_0$ ,  $A \in \mathbb{R}^{2k \times k}$  be a H-representation of  $[-1, 1]^k$ , then  $AW_\perp^T x \leq b_0$ ,  $AW_\perp^T \in \mathbb{R}^{2k \times d}$  is an H-representation of a  $d$ -dimensional polytope and  $Mx \leq b_0$ ,  $M = AW_\perp^T (GW_\perp^T)^{-1} \in \mathbb{R}^{2k \times d}$  is a H-representation of the full-dimensional, centrally symmetric polytope  $C \subset P$  with  $\leq 2k$  facets. Each  $C_i$  in MMC arises from a parallel shifting of the facets of  $C$ . This type of  $C$  improves the schedule when order is low, e.g.  $\leq 4$ .

Let  $Mx \leq b_0$ ,  $x \in \mathbb{R}^d$  the H-representation of  $C$ . We introduce a second improvement in the schedule: In each step  $i - 1$  we do not compute a  $q_i$  in an interval  $[q_{\min}, q_{\max}]$  as suggested in Section 2.1 but we consider two vectors  $b_{\min}^i, b_{\max}^i \in \mathbb{R}^{2k}$  and compute with binary search a  $t_i \in [0, 1]$  s.t.  $b^i = b_{\min}^i + t_i(b_{\max}^i - b_{\min}^i)$  and  $C_i := \{x \mid Mx \leq b^i\}$  results to successions in both **testL** and **testR**. For a  $\hat{t}_i$  if the **testL** is succeeded and **testR** is failed we continue to the right-half of the interval and if **testL** is failed and **testR** is succeeded we continue to the left-half; if both fail (contradiction) we sample a new set of  $\nu N$  points and repeat both tests.

► **Proposition 5.** Let  $A \in \mathbb{R}^{q \times d}$  the matrix that contains row-wise the normals of the facets of a convex polytope  $C \subset P$ , where  $P$  is a  $d$ -dimensional zonotope. Let  $G \in \mathbb{R}^{d \times k}$  the generators' matrix and  $r_l = AG_l$ , the  $l$ th row of  $AG$  and  $b_{\max} \in \mathbb{R}^m$  s.t.  $b_{\max}^l = \sum_{j=1}^d |r_{lj}|$ ,  $l = 1, \dots, q$ , where  $b_{\max}^l$  is the  $l$ th coefficient of  $b_{\max}$ . If  $C_{\max} := \{x \mid Ax \leq b_{\max}\}$  then  $C_{\max} \supseteq P$  holds. Moreover for every facet  $f_j$  of  $C_{\max}$ ,  $f_j \cap P \neq \emptyset$ ,  $j = 1, \dots, q$  holds.

**Proof.** Let  $G \in \mathbb{R}^{d \times k}$  the matrix of zonotope  $P$ ,  $H := \{c^T x \leq z_0\}$ ,  $c \in \mathbb{R}^d$  a halfspace intersecting  $P$ . Let  $z_{\max} = \max\{c^T y \mid y \in P\}$ . For all  $y_0 \in P$  there is a  $\lambda \in [-1, 1]^k$  s.t.  $y_0 = G\lambda$ , so  $z_{\max} = \max\{c^T G\lambda \mid \lambda \in [-1, 1]^k\}$ . The  $\lambda$  that gives the maximum inner product with a vector  $v \in \mathbb{R}^k$  is the following,

$$\lambda_i = \begin{cases} 1 & v_i \geq 0 \\ -1 & v_i < 0 \end{cases}, \quad i = 1, \dots, k$$

So  $z_{\max} = \sum_{i=1}^k |c^T G_i|$ . Then for the halfspace  $H' := \{c^T x \leq z_{\max}\}$ ,  $H' \supseteq P$  holds. Moreover  $H' \cap P \neq \emptyset$ . We apply the same for every facet of  $C \subset P$ .  $\blacktriangleleft$

Following this proposition, we use  $b_0, b_{\max}$  to compute  $C'$  in the initialization step of the schedule obtaining a vector  $b'$ . Then in each step,  $b_{\min} = b'$  and  $b_{\max} = b_{i-1}$ . When  $C'$  is an H-polytope we estimate  $\text{vol}(C_m)$  using Algorithm 1 by using balls in MMC and, moreover, we sample from  $C_m$  with HnR to estimate ratio  $r_m$ .

### 3 Implementation and experiments

In this section we discuss our implementation and setup the parameters of the algorithm. We perform extended experiments analyzing various aspects of our method such as practical complexity and how it is affected by the bodies used in MMC. Finally, we apply our software to test the quality of approximation of various methods for low order reduction of zonotopes.

We use the `eigen` library (<http://eigen.tuxfamily.org>) for linear algebra and `lpSolve` (<http://lpsolve.sourceforge.net>) for solving LPs. All experiments have been performed on a personal computer with Intel® Core i7-6700 3.40GHz × 8 CPU and 32GB RAM. All runtimes reported in the plots and tables are averaged over 10 runs unless otherwise stated. When we use balls in MMC we denote by `CoolingBall` the implementation of Algorithm 1, and by `CoolingHpoly` when we use the H-polytope from Section 2.5. We denote by `CoolingGaussian` the implementation of [7] and by `SeqOfBalls` that of [11].

**Polytope database.** To perform our experiments is vital to adopt a polytope database with polytopes that explore average cases as well as corners of our method. We use

- `cube-d`:  $\{x = (x_1, \dots, x_d) \mid x_i \leq 1, x_i \geq -1, x_i \in \mathbb{R} \text{ for all } i = 1, \dots, d\}$ ,
- `cross-d`: cross polytope, the dual of cube, i.e.  $\text{conv}(\{-e_i, e_i, i = 1, \dots, d\})$ ,
- `$\Delta$ -d`: the  $d$ -dimensional simplex  $\text{conv}(\{e_i, \text{ for } i = 1, \dots, d\})$
- `rh-d-m`: polytopes constructed by choosing  $m$  random hyperplanes tangent to the sphere,
- `rv-d-n`: dual to `rh-d-m`, i.e. polytopes with  $n$  vertices randomly distributed on the sphere,
- `z-d-k`:  $\sum_{s \in S} s$ ; choose a random direction for each segment  $s \in S$  and pick a random length in the interval  $[0, \sqrt{d}]$

In the experiments of this paper we do not apply to the polytope any rounding step before the volume computation. However, in the case of random V-polytopes, we compute the minimum volume enclosing ellipsoid of the vertices and then we apply to the polytope a linear map that maps the ellipsoid to the unit ball, to test our method for random polytopes that are near to well-rounded position (Table 1).

**Annealing Schedule.** For the cooling parameters we set  $r = 0.1$  and  $\delta = 0.05$  in order to define the next convex body in MMC with about 10% of the volume of the previous body, and we choose the significance level to be  $\alpha = 0.10$ . A smaller  $\alpha$  can be chosen for a tighter test around  $r + \delta$ . We set the number of points that are generated from  $P_i$  in each step to be  $\nu N = 1200 + 2d^2$  and  $\nu = 10$ . The value of  $\nu N$  was experimentally determined; HnR generates approximate samples, so we set  $\nu N = O(d^2)$  to obtain, in practice, the normal approximation that Remark 2.1 implies. The choice of these parameters might be improved in the future. In the  $i$ -th step of the schedule we sample from  $P_i$  and then check if the stopping criterion holds. If it fails we binary search reusing the sample. Hence we sample only once a set of  $\nu N$  points from  $P_i$  in each step of Algorithm 2.

When  $C$  is a ball we can sample almost perfectly uniform points from it (no need of random walks). Following Remark 2.1, the normal approximation suffices when  $r_i = 0.1$  and  $N = 112$ , thus we set  $\nu N = 1200 = O(1)$ ,  $\nu = 10$ . When  $C$  is the polytope of Section 2.5 we set a large step for HnR, namely  $10 + 2d$ , to get more accurate samples, and set  $\nu N = 1200$  as we can assume that the sample is close to uniform. For the rest of the steps in the schedule we use HnR to sample from  $P_i$  where the value  $1200 + 2d^2$  was picked experimentally so that we have stable cooling as the dimension grows.

## 14 Practical volume estimation

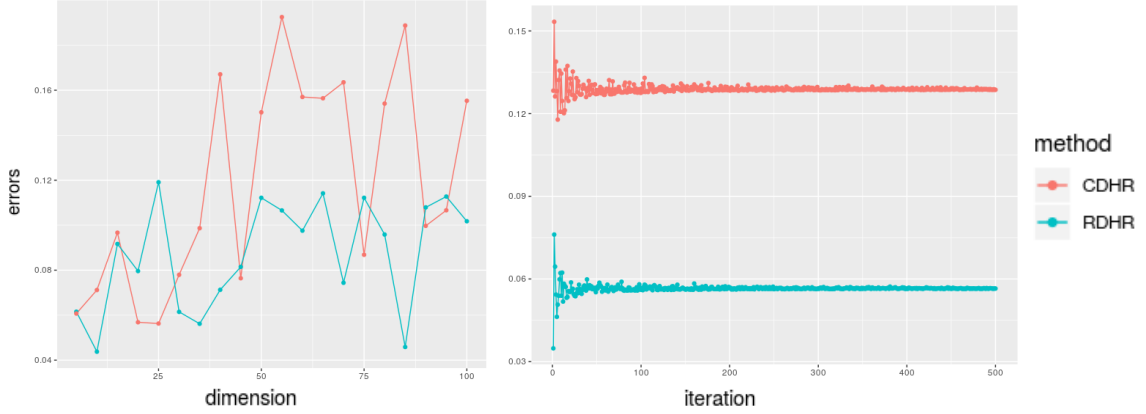
When using balls, let  $C$  be the unit ball, then  $q_{\min}, q_{\max}$  are minimum and maximum radii in computing  $C'$ . We set  $q_{\min} = 0$  and sample  $1200 + 2d^2$  points to set  $q_{\max}$  s.t. all points belong to  $q_{\max}C$ . For low order zonotopes we use the polytope in Section 2.5 and follow those steps.

Experimental results for V-polytopes.							
$P$	Vol	m	steps	error	time	ex. Vol	ex. time
cross-20	4.54e-13	1	3.42e+03	0.05	2.81	--	--
cross-40	1.22e-36	1	8.23e+03	0.09	14.5	--	--
cross-60	1.27e-64	1	20.6e+03	0.08	60.1	--	--
cross-80	1.62e-95	1	29.3e+03	0.04	122	--	--
cross-100	1.43e-128	2	94.2e+03	0.05	406	--	--
$\Delta$ -20	4.24e-19	2	1.49e+04	0.03	6.970	4.11e-19	0.07
$\Delta$ -40	1.32e-48	5	21.2e+04	0.08	210.3	1.22e-48	0.008
$\Delta$ -60	1.08e-82	10	77.4e+04	0.1	1442	1.203e-82	0.02
$\Delta$ -80	1.30e-119	13	187e+04	0.07	6731	1.39e-119	0.07
cube-10	1052.4	1	1851	0.03	54.39	--	--
cube-11	1930.2	1	1935	0.06	155.9	--	--
cube-12	4240.6	1	2017	0.04	567.0	--	--
cube-13	7538.2	1	2127	0.08	2937	--	--
rv-10-20	9.11e-06	1	0.185e+04	0.08	1.57	9.87e-06	0.015
rv-10-40	5.04e-04	1	0.185e+04	0.09	1.92	4.64e-04	0.46
rv-10-80	3.74e-03	1	0.185e+04	0.08	3.35	3.46e-03	6.8
rv-10-160	1.59e-02	1	0.140e+04	0.06	5.91	1.50e-03	59
rv-15-30	2.73e-10	1	0.235e+04	0.02	3.46	2.79e-10	2.1
rv-15-60	4.41e-08	1	0.235e+04	??	6.46	--	--
rv-20-40	1.27e-15	1	0.305e+04	??	6.24	--	--
rv-30-60	6.06e-28	1	0.914e+04	??	25.7	--	--
rv-40-80	9.37e-42	2	3.02e+04	??	148	--	--
rv-50-100	8.34e-57	2	4.29e+04	??	325	--	--
rv-20-200	2.57e-10	1	0.305e+04	??	35.3	--	--
rv-20-2000	2.89e-07	1	0.305e+04	??	457	--	--
rv-80-160	5.84e-106	3	11.3e+04	??	325e+01	--	--
rv-100-200	1.08e-141	4	24.5e+04	??	133e+02	--	--

■ **Table 1** Vol: the average estimated volume; m: the maximum number of phases in MMC; steps: the average number of steps of `CoolingBall`; error: the error of each computation; time: the average time in seconds for `CoolingBall`; ex. Vol: the exact volume; ex. time: the time in seconds for the exact volume computation i.e. `qhull` in R (package `geometry`). The -- implies that the execution failed due to memory issues or exceeded 1 hr. We set the requested error  $\epsilon = 0.1$  for all the above.

**Error splitting.** We do not split the error equally to all ratios, but set  $\epsilon_m = \epsilon/2\sqrt{m+1}$  in order to be the smallest one as the ratio  $\text{vol}(P_m)/\text{vol}(C_m)$  converges faster than the other ratios in practice. The latter occurs because sampling from  $C_m$  is usually faster and more accurate, e.g. when  $C_m$  is a ball. Then we split  $\epsilon' = \epsilon\sqrt{4(m+1)-1}/2\sqrt{m+1}$  equally to the remaining ratios, i.e.  $\epsilon_i = \epsilon'/\sqrt{m}$ ,  $i = 0, \dots, m-1$  so that Equation (2) holds. As we mentioned in section 2.5, if  $C_m$  is an H-polytope and  $P$  a zonotope we estimate  $\text{vol}(C_m)$  calling Algorithm 1 and by using balls in MMC. For the computation of  $\text{vol}(C_m)$  we set  $\epsilon'' = \epsilon/2\sqrt{m+1}$  and then we equally split  $\epsilon' = \epsilon\sqrt{2m+1}/\sqrt{2m+2}$  to the  $m+1$  ratios respecting Equation (2).

**Sliding window.** For the ratio estimation we reuse the points from annealing schedule but we



■ **Figure 2** Left: the errors of `CoolingBall` using RDHR and CDHR for unit cubes in H-representation,  $d = 5, 10, \dots, 100$ . Right: We run `CoolingBall` multiple times. The plot shows the errors of `CoolingBall` averaged in each iteration using RDHR and CDHR for the 20-dimensional unit cube in H-representation as well; RDHR converges to 0.057 and CDHR converges to 0.129.

use only the value of the ratio between the number of successes over  $\nu N$ . For the sliding window length, set  $k = 2d^2 + 250$  since our experiments on the error show this choice offers stability. In Figure 2 we see that, for unit cubes, the error of Algorithm 1 when  $\epsilon = 0.1$  is around that value and converges to 0.057 while we increase the number of experiments and take the average error for the 20-dimensional unit cube. If we set  $k = O(d)$  the error of our method seems to exceed  $\epsilon$  while the dimension increases, but we believe further improvements can be made. For each new generated point we update the mean and the variance of the sliding window in  $O(1)$  instead of  $O(d)$ : Let  $\hat{\mu}$  be the mean of the sliding window, then we write the sample variance,

$$\frac{1}{k} \sum_{i=1}^k (\hat{r}_i - \hat{\mu})^2 = \frac{1}{k} \left( \sum_{i=1}^k \hat{r}_i^2 - 2\hat{\mu} \sum_{i=1}^k \hat{r}_i + k\hat{\mu}^2 \right)$$

We store the sum of the window's ratios and the sum of the squared ratios. For each new generated point we obtain an updated ratio and the oldest ratio is popped out. We use both values to update both  $\sum_{i=1}^k \hat{r}_i^2$  and  $\sum_{i=1}^k \hat{r}_i$  and to compute the updated mean value and st.d. of the window. In practice the length of the window is always small enough to achieve numerical robustness.

**Sampling by HnR.** Theoretical bounds for the mixing time are too pessimistic, thus our approach is more aggressive and we set the step equals to one. Moreover we do not compute a warm start for the random walk; we always start HnR from the feasible point we compute in  $P$  when we estimate ratio  $r_i$ . This approach is faster because the sliding window can handle efficiently these disadvantages. For zonotopes and V-polytopes we use RDHR since coordinate directions do not have any advantage. When  $P$  is a H-polytope we use CDHR but our experiments show that RDHR is statistically more stable as you can see in Figure 2.

**Body selection for MMC.** Algorithm 1 needs a point in  $P$  in order to start the sampling. If  $P$  is an H-polytope we compute the Chebychev center [4]. When  $P$  is a zonotope we use the origin. For V-polytopes, we compute an approximation of the minimum volume enclosing ellipsoid and use the center of the ellipsoid as a feasible point. In general, for zonotopes, one selects convex body  $C$  as follows: Estimate  $\text{vol}(C' \cap P)$  for  $C$  being a ball and the H-polytope in Section 2.5; according to Corollary 4 pick the one that maximizes this volume.

Figure 3 shows that for random zonotopes of order  $\leq 4$ , if we use the H-polytope, the number of bodies used in MMC is smaller for all pairs  $(d, k)$  compare to the case of using balls. Notice that, when we use balls in MMC, the number of phases is decreasing for a constant  $d$  while  $k$  increases. Table 2 shows that the number of phases for high-order zonotopes is  $m = 1$ , whereas for low-order



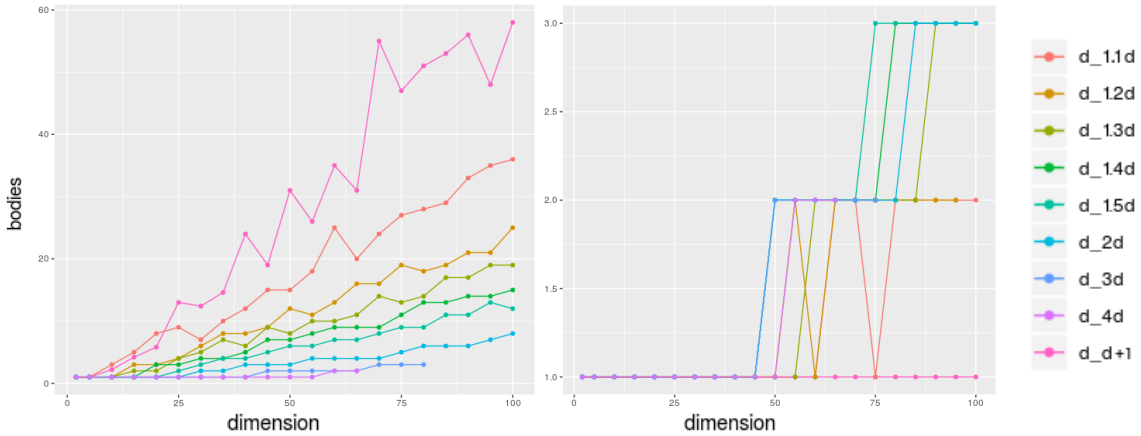


**Figure 3** Left: Number of bodies in MMC using balls. Right: Number of bodies in MMC using centrally symmetric H-polytopes. We set the number of generators  $k = d + 1$ ,  $[1.1d]$ ,  $[1.2d]$ ,  $[1.3d]$ ,  $[1.4d]$ ,  $[1.5d]$ ,  $2d$ ,  $3d$ ,  $4d$  and we generate a random zonotope for each experiment.

zonotopes the H-polytope we defined reduces significantly the number of phases and runtime. The maximum number of phases for zonotopes (up to what our software computes in  $< 10\text{hr}$ ) is  $m \leq 3$ .

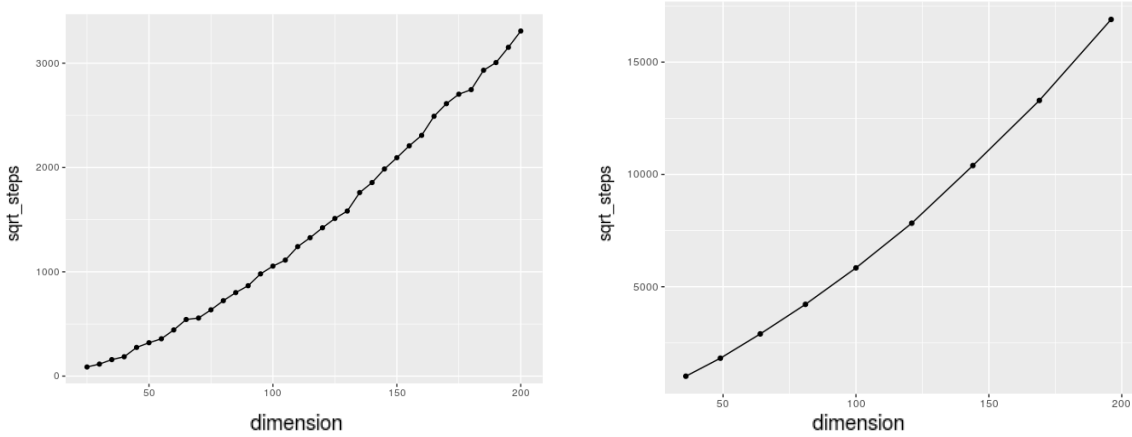


**Figure 4**  $\sqrt{\#\text{steps}}$  as a function of  $d$  for unit cubes (left) and Birkhoff polytopes (right). Left: the dimension  $d = 5, 10, \dots, 200$ . Right:  $n = 7, 4, \dots, 15$  for Birkhoff polytopes  $B_n$ . We use balls in MMC.

**Experimental complexity.** To study practical complexity we experimentally correlate the total number of HnR steps  $n$  with  $d$ . Then, runtime grows accordingly to the cost of each step of HnR. We test unit H-cubes, Birkhoff H-polytopes, and cross V-polytopes, and found a linear relation between  $\sqrt{n}$  and  $d$  (Figures 4 and 5). The Pearson correlation coefficients between  $\sqrt{n}$  and  $d$  are  $p_1 = 0.991$ ,  $p_2 = 0.994$  and  $p_3 = 0.957$  respectively. These coefficients imply almost perfect positive linear correlation for all cases. We conclude that our method needs  $O(d^2)$  steps for these polytopes. In Figure 5 (left) notice that for  $d \leq 85$  our method defines only one ball in MMC for the cross polytope while for  $d = 100$  it defines two balls, thus verifying the observation in Section 2.4 for the particular polytope. In Table 1 notice that the maximum number of phases for random V-polytopes after rounding is  $\leq 4$ , showing that our method defines just a few rejection sampling steps for random convex polytopes that are near to well-rounded position for  $d \leq 100$ .

**Comparison with other implementations.** We compare against the (only) two available implementations for high dimensional volume estimation namely, the `matlab` implementation of

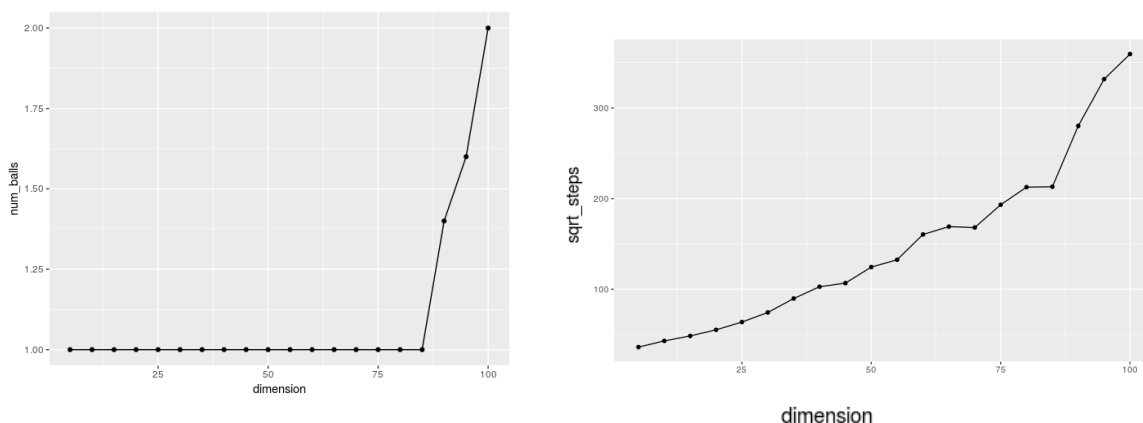
Experimental results for zonotopes.						
$z-d-k$	<i>Body</i>	<i>order</i>	<i>Vol</i>	<i>m</i>	<i>steps</i>	<i>time</i>
z-5-500	Ball	100	4.63e+13	1	0.1250e+04	22.26
z-10-1000	Ball	100	2.62e+29	1	0.1400e+04	130.1
z-15-1500	Ball	100	5.00e+45	1	0.1650e+04	506.1
z-20-2000	Ball	100	2.79e+62	1	0.2000e+04	1428
z-50-65	Hpoly	1.3	1.42e+62	1	1.487e+04	173.9
z-60-78	Hpoly	1.3	2.88e+75	2	3.800e+04	529.5
z-70-91	Hpoly	1.3	7.64e+90	2	5.470e+04	1067
z-80-104	Hpoly	1.3	1.10e+107	2	8.685e+04	2277
z-90-117	Hpoly	1.3	1.76e+122	3	10.17e+04	2810
z-100-130	Hpoly	1.3	1.37e+138	3	17.19e+04	6073
z-40-60	Hpoly	1.5	4.23e+51	1	0.7851e+04	104.5
z-45-67	Hpoly	1.5	4.17e+58	1	0.9551e+04	135.0
z-50-75	Hpoly	1.5	2.96e+66	2	1.615e+04	253.6
z-55-82	Hpoly	1.5	9.83e+74	2	3.469e+04	541.2
z-60-90	Hpoly	1.5	5.81e+82	2	5.355e+04	943.9
z-65-97	Hpoly	1.5	1.40e+90	2	4.869e+04	1296
z-70-105	Hpoly	1.5	8.66e+98	2	5.495e+04	1352
z-75-112	Hpoly	1.5	1.45e+107	3	4.915e+04	1632
z-80-120	Hpoly	1.5	8.48e+114	3	12.35e+04	4180
z-85-127	Hpoly	1.5	1.04e+123	3	12.09e+04	4507
z-90-135	Hpoly	1.5	5.11e+131	3	14.44e+04	6710
z-95-142	Hpoly	1.5	2.21e+141	3	15.55e+04	8524
z-100-150	Hpoly	1.5	2.32+149	3	15.43e+04	10060
z-70-140	Hpoly	2	8.71e+111	2	5.059e+04	2695
z-75-150	Hpoly	2	6.18e+121	3	11.12e+04	4036
z-80-160	Hpoly	2	2.01e+131	3	11.31e+04	5356
z-100-200	Hpoly	2	5.27e+167	3	15.25e+04	34110

■ **Table 2** *Body* stands for the type of body in MMC; *order* =  $k/d$ , *Vol* the average of volumes by `CoolingHpoly` over 10 runs; *m* the maximum number of phases; *steps* is the number of steps; *time* is average time in seconds;  $\epsilon = 0.1$  except for z-80-160 and z-100-200 where  $\epsilon = 0.2$ .

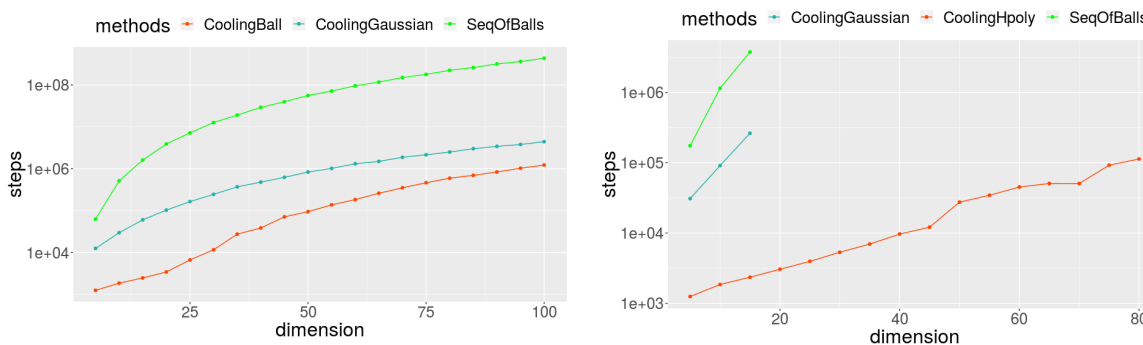
`CoolingGaussian` and the C++ implementation of `SeqOfBalls`. In Table 3 we use the matlab implementation `CoolingGaussian` for the number of steps. For more fair time comparisons we implement in C++ the method of `CoolingGaussian`. Interestingly, we found our implementation to be around 10 times faster; then we compare the performance of the two C++ implementations in Table 3. The experimental results in Table 3 show that `CoolingBall` is faster than both `CoolingGaussian` and `SeqOfBalls` for  $d \leq 100$  and for the 120 dimensional hypercube. Figure 6 (left plot) shows the number of steps of `CoolingBall`, `CoolingGaussian` and of `SeqOfBalls` on unit H-cubes. In [7] they show that the number of steps `CoolingGaussian` needs is  $O(d^2)$  even for unit cubes. Our experiments confirm this complexity and show that `CoolingBall` is faster than `CoolingGaussian` for  $d \leq 100$  and asymptotically faster than `SeqOfBalls`.

To compare `CoolingGaussian` and `SeqOfBalls` with Algorithm 1 for zonotopes we define an inscribed ball and for `CoolingGaussian` we give the known upper bound on the number of facets.

## 18 Practical volume estimation



■ **Figure 5** Left: Number of balls in MMC for cross polytopes. Right: The  $\sqrt{\#\text{steps}}$  for cross polytopes. In both plots,  $d = 5, 10, \dots, 100$ .



■ **Figure 6** Left: the number of steps for for unit cubes in H-representation,  $d = 5, 10, \dots, 100$ . Right: the number of steps for random zonotopes of order 2,  $d = 5, 10, \dots, 80$ . In both plots we use  $\log_{10}$  scale for the  $y$ -axis

We compute  $r = \max\{\gamma \mid \gamma e_i \in P\}$ , then the ball  $B(\mathbf{0}, r/\sqrt{d}) \subseteq P$ . In Figure 6 (right plot) we compare the number of steps for random zonotopes of order 2, between `CoolingHpoly` and both `CoolingGaussian` and `SeqOfBalls`. `CoolingGaussian` fails to estimate volumes for  $d > 15$  as the upper bound for the number of facets is the bottleneck for this implementation while `SeqOfBalls` takes  $> 1$  hr for  $d > 15$ . Moreover `CoolingHpoly` needs a smaller number of steps for  $d = 80$  than `CoolingGaussian` for a random zonotope in  $d = 15$ . In Table 1 we give volume estimations for V-polytopes and exact computation using `qhull`. Notice `CoolingBall` scales efficiently up to  $d = 100$  for random V-polytopes after the rounding step we described. Moreover, it is very efficient for the case of cross polytope while `qhull` fails for  $d \geq 20$ . In addition, `CoolingBall` estimates the volume of the hypercube for  $d \leq 13$  and takes  $\geq 1$  hr for larger dimensions as the number of vertices grows exponentially in  $d$ . Finally, notice that `qhull` is faster for simplices as the computation of the convex hull is very fast.

Summarizing our implementations of Algorithm 1 for V-polytopes and zonotopes outperforms both `CoolingGaussian` and `SeqOfBalls` and, additionally, perform volume computations which were intractable until now. `CoolingBall` is asymptotically better than `SeqOfBalls` and faster for  $d \leq 100$  than `CoolingGaussian` for H-polytopes.

Experimental results for H-polytopes.													
$P$	cB Vol	m	cB steps	cB error	cB time	cG Vol.	cG steps	cG error	cG time	SoB Vol.	SoB steps	SoB error	SoB time
cube-20	1.06e+05	1	0.0419e+05	0.01	0.10	9.94e+05	0.997e+05	0.05	0.030	1.05e+06	0.363e+07	0.002	1.32
cube-40	9.91e+11	2	0.347e+05	0.09	0.20	1.13e+12	5.31e+05	0.03	0.24	1.15e+12	2.84e+07	0.05	16.5
cube-60	1.23e+18	5	2.05e+05	0.07	0.63	1.24e+18	12.8e+05	0.07	0.70	1.19e+18	9.42e+07	0.03	58.6
cube-80	1.27e+24	7	5.37e+05	0.05	1.6	1.16e+24	26.7e+05	0.04	4.1	1.22e+24	22.2e+07	0.02	156
cube-100	1.23e+30	9	10.8e+05	0.03	3.7	1.34e+30	45.5e+05	0.05	9.4	1.17e+30	43.3e+07	0.08	301
cube-120	1.25e+36	12	20.1e+05	0.06	7.1	1.19e+36	83.8e+05	0.1	14	1.37e+36	75.1e+07	0.03	897
$\Delta$ -60	1.07e-82	11	10.7e+05	0.02	0.99	1.26e-82	22.1e+05	0.04	2.9	1.15e-82	21.6e+07	0.04	70.2
$\Delta$ -80	5.46e-113	16	42.3e+05	> 1	2.9	1.39e-119	45.9e+05	0.003	6.4	1.46e-119	0.876e+07	0.04	173
* $\Delta$ -80	1.31e-119	16	29.0e+05	0.06	35	1.39e-119	45.9e+05	0.003	6.4	1.46e-119	0.876e+07	0.04	173
$\Delta$ -100	2.65e-149	21	92.4e+05	> 1	7.4	1.13e-158	79.9e+05	0.05	16	1.06e-158	1.35e+07	0.01	528
* $\Delta$ -100	9.80e-159	21	55.2e+05	0.06	90	1.13e-158	79.9e+05	0.05	16	1.06e-158	1.35e+07	0.01	528
rh-20-60	2.66e+27	3	0.259e+05	??	0.074	2.35e+27	1.83e+05	??	0.16	2.44e+27	0.449e+07	??	3.24
rh-40-160	3.82e+53	5	1.82e+05	??	0.47	2.66e+53	7.51e+05	??	1.8	2.52e+53	3.14e+07	??	5.54
*rh-40-160	2.26e+53	5	2.07e+05	??	2.5	2.66e+53	7.51e+05	??	1.8	2.52e+53	3.14e+07	??	5.54
rh-60-300	5.68e+77	7	5.14e+05	??	2.1	5.68e+77	16.8e+05	??	6.8	6.10e+77	9.48e+07	??	305
rh-100-600	7.68e+126	1	19.0e+05	??	13	7.40e+126	59.0e+05	??	51	–	–	–	> 1 hr

■ **Table 3**  $P$  the type of polytope;  $m$  for the maximum number of phases in MMC among 10 experiments for `CoolingBall`. `cb` denotes `CoolingBall`, `cg` denotes `CoolingGaussian` and `SoB` denotes `SeqOfBalls`. *Vol* the averaged estimated volume, *steps* the averaged number of steps, *error* the error of each method, *time* the averaged time in seconds. The \* denotes that we use RDHR where CDHR for `CoolingBall` fails. We set the requested error  $\epsilon = 0.1$  for all the above.

### 3.1 Application: test zonotope approximations

We propose an efficient algorithm for evaluating over-approximation of a zonotope  $P$ . Zonotopes are critical in applications such as autonomous driving [1] or human-robot collaboration [20]. Algorithm complexity strongly depends on the order of the encountered zonotopes. Thus, a practical solution is to over-approximate  $P$ , as tight as possible, with another zonotope  $P_{red} \supseteq P$  of smaller order. A good measure of the approximation’s quality (fitness) is

$$R = (\text{vol}(P_{red})/\text{vol}(P))^{1/d}. \quad (6)$$

This reduces to volume computation. In [14] they compute volumes exactly and deterministically, therefore they cannot compute the quality of approximation for  $d > 10$ .

Here, we employ our software to test the quality of such approximations. Methods that are able to scale for  $d \geq 20$  are, primarily, Principal Component Analysis (PCA) and the BOX method [14]. Both adopt similar approximations and are of comparable reliability; here we focus on PCA.

**PCA** (zonotope  $P$  with generators’ matrix  $G \in \mathbb{R}^{d \times k}$ )  
 $X = [G | -G]^T$   
 $USV^T = \text{SVD}(X^T X)$   
**Return:**  $G_{red} = U \cdot IH(U^T G)$

Notice that  $G_{red} = U \cdot IH(U^T G)$  is square and generates  $P_{red}$ ; the  $IH(\cdot)$  is the “interval hull” from [15]. Over-approximation can be seen as a reduction problem, so that the covariance among the  $d$  generators of  $P_{red}$  must be null.

Table 4 shows experimental results for zonotopes up to  $d = 30$  of order up to 15. We use balls in MMC (`CoolingBall`);  $\text{vol}(P_{red})$  is obtained exactly by computing one determinant. For PCA over-approximations we show that  $R$  increases as  $d$  grows but the same does not occur for fixed  $d$  as order increases. This is probably the first time practical volume estimation is used to test approximation methods.

Testing ratios of PCA approximations.					
$z-d-k$	Order	$\text{vol}(P)$	Time	$\text{vol}(P_{red})$	$R$
z-10-50	5	1.19e+16	2.10	7.09e+18	1.90
z-10-100	10	1.93e+19	3.11	6.51e+21	1.79
z-10-150	15	1.24e+21	6.84	5.41e+23	1.84
z-10-500	50	1.90e+26	37.5	9.87e+28	1.86
z-15-65	5	4.21e+25	7.11	4.72e+30	2.17
z-15-150	10	8.29e+30	14.8	3.11e+35	2.02
z-15-225	15	3.46e+33	26.3	2.19e+38	2.09
z-15-750	50	1.36e+41	113	1.39e+46	2.16
z-20-200	10	5.25e+42	36.7	8.58e+49	2.29
z-20-300	15	1.78e+46	66.4	2.55e+53	2.28
z-30-300	10	1.46e+66	180	1.15e+80	2.91
z-30-450	15	6.57e+71	359	2.62e+85	2.84

■ **Table 4**  $\text{vol}(P)$  is the estimated volume of zonotope  $z-d-k$  with `CoolingBall`, in Time (sec), with requested error  $\epsilon = 0.1$ ;  $\text{vol}(P_{red})$  is the volume of the over-approximation;  $R$  the ratio of fitness in Equation (6).

## 4 Acknowledgements

I.Z.E. and A.C. are partially supported by the European Union’s Horizon 2020 research and innovation programme under grant agreement No 734242 (Project LAMBDA). We would like to thank Prof. Althoff for discussions on zonotope approximation methods (Section 3.1).

---

## References

- 1 M. Althoff and J. M. Dolan. Online verification of automated road vehicles using reachability analysis. *IEEE Transactions on Robotics*, 30(4):903–918, Aug 2014.
- 2 U. Betke and M. Henk. Approximating the volume of convex bodies. *Discrete & Computational Geometry*, 10:15–21, 1993.
- 3 J. Bourgain and J. Lindenstrauss. Approximating the ball by a Minkowski sum of segments with equal length. *Discrete Computational Geometry*, 9:131–144, 1993.
- 4 Stephen Boyd and Lieven Vandenbergh. *Convex Optimization*. Cambridge University Press, New York, NY, USA, 2004.
- 5 A. Chevallier, S. Pion, and F. Cazals. Hamiltonian Monte Carlo with boundary reflections, and application to polytope volume calculations. Research Report RR-9222, INRIA Sophia Antipolis, France, 2018.
- 6 B. Cousins and S. Vempala. Bypassing KLS: Gaussian cooling and an  $O^*(n^3)$  volume algorithm. In *Proc. ACM STOC*, pages 539–548, 2015.
- 7 B. Cousins and S. Vempala. A practical volume algorithm. *Mathematical Programming Computation*, 8, June 2016.
- 8 H. Cramer. *Mathematical methods of statistics*. Princeton University Press, 1946.
- 9 M. Dyer, A. Frieze, and R. Kannan. A random polynomial-time algorithm for approximating the volume of convex bodies. *J. ACM*, 38(1):1–17, 1991.
- 10 G. Elekes. A geometric inequality and the complexity of computing volume. *Discr. Comput. Geom.*, 1(4):289–292, 1986.

- 11 I.Z. Emiris and V. Fisikopoulos. Practical polytope volume approximation. *ACM Trans. Math. Soft.*, 44(4):38:1–38:21, 2018. Prelim. version: Proc. Symp. Comp. Geometry, 2014.
- 12 Komei Fukuda. Frequently asked questions in polyhedral computation. <ftp://ftp.math.ethz.ch/users/fukudak/reports/polyfaq040618.pdf>, 2004.
- 13 E. Gover and N. Krikorian. Determinants and the volumes of parallelotopes and zonotopes. *Linear Algebra and its Applications*, 413:28–40, 2010.
- 14 A.K. Kopetzki, B. Schürmann, and M. Althoff. Methods for order reduction of zonotopes. pages 5626–5633, 2017.
- 15 W. Kühn. Rigorously computed orbits of dynamical systems without the wrapping effect. *Computing*, 61:47–67, 1998.
- 16 Y.T. Lee and S. Vempala. Convergence rate of Riemannian Hamiltonian Monte Carlo and faster polytope volume computation. In *Proceedings of the 50th Annual ACM SIGACT Symposium on Theory of Computing*, STOC 2018, pages 1115–1121, 2018.
- 17 L. Lovász, R. Kannan, and M. Simonovits. Random walks and an  $O^*(n^5)$  volume algorithm for convex bodies. *Random Structures and Algorithms*, 11:1–50, 1997.
- 18 L. Lovász and S. Vempala. Simulated annealing in convex bodies and an  $O^*(n^4)$  volume algorithms. *J. Computer and System Sciences*, 72:392–417, 2006.
- 19 K.G. Murty. Ball centers of special polytopes. *Department of Industrial and Operations Engineering, University of Michigan*, 2009.
- 20 A. Pereira and M. Althoff. Safety control of robots under computed torque control using reachable sets. In *2015 IEEE International Conference on Robotics and Automation (ICRA)*, pages 331–338, May 2015.